Electronic Supplementary Material (ESI) for Nanoscale Horizons.


# SUPPORTING INFORMATION

## A Selenoureido-iminoglycolipid transported by Zeolitic-Imidazolate Framework Nanoparticles: A Novel Antioxidant Therapeutic Approach

*Fátima Guerrero,[a] Andrés Carmona,[a] Victoria Vidal,[a] Ana Franco,[b] Alejandro Martín-Malo,[a] Elena M. Sánchez-Fernández*[c] and Carolina Carrillo-Carrión*[d]*

[a] *Institute Maimonides Biomedical Research Institute of Cordoba (IMIBIC), Reina Sofia University Hospital, 14004 Córdoba, Spain.*
[b] *Leibniz Institute für Katalyse e.V., 18059 Rostock, Germany.*
[c] *Department of Organic Chemistry, Faculty of Chemistry, University of Seville. C/ Profesor García González 1, 41012 Sevilla, Spain. E-mail: esanchez4@us.es*
[d] *Institute for Chemical Research (IIQ), CSIC-University of Seville. Avda. Américo Vespucio 49, 41092 Sevilla, Spain. E-mail: carolina.carrillo@csic.es*

**TABLE OF CONTENTS**

## S1. General information

**Chemicals and prepared compounds:** All reagents were obtained from commercial sources and used without further purification. Thin-layer chromatography was performed on precoated TLC plates, silica gel 30F-245, with visualization by UV light and by carrying with 10% $H_2SO_4$ or 0.2% w/v cerium (IV) sulphate-5% ammonium molybdate in 2M $H_2SO_4$ or 0.1% ninhydrin in EtOH. Column chromatography was performed on Chromagel (silice 60 AC.C 70-200 μm). All compounds were ≥95% purity as determined by elemental microanalysis performed on a LECO CHNS-932 analyzer (IIQ, CSIC-US). The analytical results for C, H, N, and S were within ± 0.4 of the theoretical values.

**Nuclear Magnetic Resonance Spectroscopy (NMR)**: $^{1}H$ ($^{13}C$) NMR spectra were performed on Bruker Avance spectrometers at 300 and 500 MHz (75.5, 125.7). 2-D COSY and HSQC experiments were carried out to assist on NMR assignments.

**High-performance liquid chromatography coupled with mass spectrometry (HPLC-MS):** HPLC-MS analyses were done using a Waters Alliance 2695 HPLC coupled to an ESI-ion trap mass spectrometer instrument (Bruker AmaZon). Samples were analyzed using 0.1% formic acid eluting gradients at a flow rate of 0.3 mL/min. Spectra were registered in both positive and negative modes and the results were processed using equipped with Compass HyStar software in the *m/z* 100-2000 range.

**Optical rotations:** Measurements were performed with a JASCO P-2000 polarimeter using a sodium lamp (λ = 589 nm) at 20 ± 2 ºC in 1 cm or 1 dm tubes.

**Transmission Electron Microscopy (TEM):** TEM images were acquired using a JEOL 2100Plus operated at 200 kV. Samples were prepared by drying a diluted dispersion of the particles on 200 mesh copper grids coated with Formvar/carbon film.

**Scanning Electron Microscopy (SEM):** SEM images were acquired using a HITACHI S4800 field emission microscope operating at 2 kV in secondary electron and backscattered electron modes. Samples were prepared by drying, under ambient conditions, a diluted dispersion of the particles on a silicon wafer substrate. Elemental composition was analysed by Energy Dispersive X-Ray Analysis (EDX) using the same SEM instrument with an integrated Bruker AXS Microanalysis QUANTAX EDX system.

**Dynamic Light Scattering (DLS) and Zeta-Potential (ζ-potential):** Measurements were performed using a Malvern Zetasizer Nano ZSP equipped with a 10 mW He–Ne laser operating at a wavelength of 633 nm and fixed scattering angle of 173˚. For DLS analysis, diluted samples were loaded into a quartz cuvette and then three measurements, each consisting of twelve data runs, were taken at room temperature after an equilibration step of 120 sec. The ζ-potential of samples in aqueous solutions were measured with laser Doppler anemometry (LDA) by using the same instrument.

**Powder X-Ray Diffraction (PXRD):** X-ray analysis of samples in powder form was performed using a Bruker D8-Advance Diffractometer. X-ray radiation of Cu Kα was used and the measurement range was 5°–50° (2θ) with a step of 0.03°.

**$N_2$ physisorption analysis**: $N_2$ sorption isotherms were carried out at 77 K on a a Micromeritics Tristar II 3020 system. Before analysis, samples were degassed under vacuum for 18 h at 120 °C. The apparent surface area was calculated from the Brunauer–Emmett–Teller (BET) method in the pressure interval $P/P_0$ =0.01-0.3. Pore volume and external surface area were determined by the t-plot method.

**Absorbance**: Colorimetric viability assays in cells were performed on a PowerWave XS Microplate Spectrophotometer.

**Fluorescence**: For ROS analyses in cells, the fluorescence measurements were performed at $\lambda_{ex/em}$ = 485/535 nm using a Tecan Infinite 200 PRO Microplate reader.

**Optical Microscope**: An optical inverted OPTIKA microscope was used for the routine living cell examinations, as well as for the angiogenesis and wound healing assays to take cell images required for further analyses.

**Confocal Microscopy**: Images were obtained using a LSM710 confocal laser-scanning microscope (Carl Zeiss). After doing a maximum projection with the Z-stack, they were further analyzed using the imaging software Aivia v12 (Leica Microsystems). Cells were segmented using the Cellpose plug-in included in the software.

## S2. Preparation of the Se-containing sp2-IGL compound (DSeU)

### S2.1. Synthetic scheme for the preparation of DSeU

The $sp^2$-iminosugar (1*R*)-1,2,3,4-tetra-*O*-acetyl-5*N*,6*O*-oxomethylidenenojirimycin (**1**)[1] was prepared according to previously reported procedure.

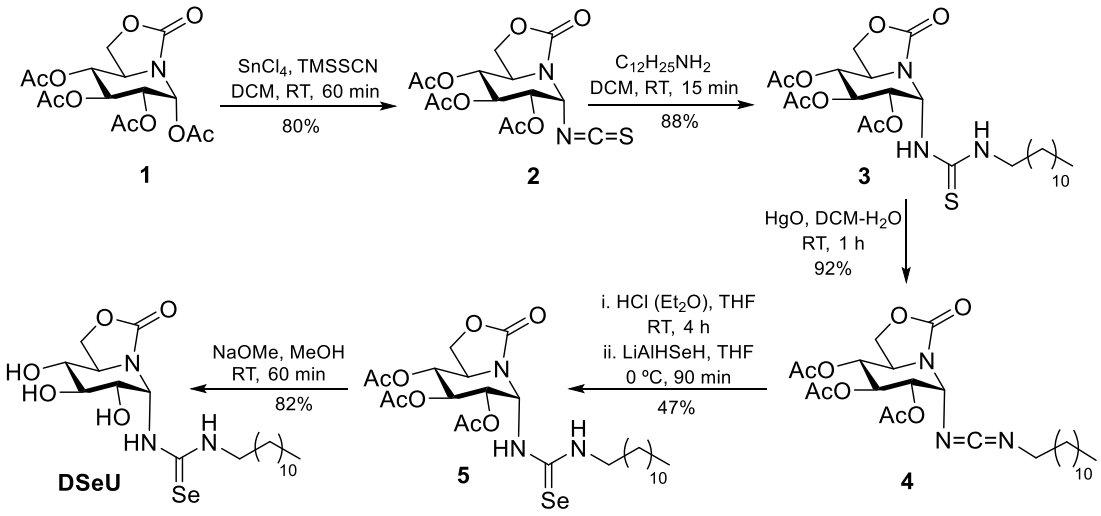


**Figure S1.** Scheme of the stereoselective synthesis of (1*S*)-(*N*'-dodecylselenoureido)-5*N*,6*O*-oxomethylidenenojirimycin (**DSeU**).

### S2.2. Synthetic procedure and structural characterization of compounds

**(1*R*)-2,3,4-Tri-*O*-acetyl-1-isothiocyanate-5*N*,6*O*-oxomethylidene-1-deoxynojirimycin (2).** A solution of the corresponding per-*O*-acetylated carbamate derivative **1**[1] (100 mg, 0.27 mmol) and tin tetrachloride ($SnCl_4$) (1 M in dichloromethane (DCM, 270 µL) in 4 mL of anhydrous DCM was stirred for 5 min. Then, trimethylsilyl isothiocyanate (TMSSCN) (42 µL, 0.29 mmol) was added and the reaction mixture was stirred at room temperature (RT) for 60 min. Saturated aqueous solution of $NaHCO_3$ (2 x 45 mL) was added and the aqueous phase was extracted with DCM (3 x 45 mL). The organic layer was washed with water (30 mL), dried ($MgSO_4$), filtered and concentrated under reduced pressure. The resulting residue was purified by column chromatography (1:1 EtOAc-cyclohexane) to afford **2**. Yield: 80 mg (80%). $R_f$ 0.67 (1:1 EtOAc-petroleum ether). $[\alpha]_D$ +79.6 (*c* 1.0 in $CHCl_3$). $^1$H NMR (500 MHz, $CDCl_3$) δ 6.09 (d, 1 H, $J_{1,2}$ = 4.5 Hz, H-1), 5.51 (t, 1 H, $J_{2,3}$ = $J_{3,4}$ = 10.0 Hz, H-3), 5.02 (dd, 1 H, H-2), 4.95 (t, 1 H, $J_{4,5}$ = 10.0 Hz, H-4), 4.49 (dd, 1 H, $J_{6a,6b}$ = 9.5 Hz, $J_{5,6a}$ = 8.0 Hz, H-6a), 4.30 (dd, 1 H, $J_{5,6b}$ = 8.0 Hz, H-6b), 4.03 (dt, 1 H, H-5), 2.17-2.09 (3 s, 9 H, MeCO). $^{13}$C NMR (125.7 MHz, $CDCl_3$) δ 170.0-169.5 (Me*CO*), 154.4 (CO), 145.2 (CS), 71.8 (C-4), 70.2 (C-2), 69.0 (C-3), 66.8 (C-6), 63.3 (C-1), 52.3 (C-5), 20.5-20.3 (*Me*CO). ESIMS: *m/z* 394.9 $[M + Na]^+$. Anal. Calcd for $C_{14}H_{16}N_2O_8S$: C 45.16, H 4.33, N 7.52, S 8.61. Found: C 45.15, H 4.22, N 7.26, S 8.33.

[1] V. M. Díaz Pérez, M. I. García Moreno, C. Ortiz Mellet, J. Fuentes, J. C. Díaz Arribas, F. J. Cañada, J. M. García Fernández, *J. Org. Chem.* **2000**, *65*, 136.

**(1*S*)-2,3,4-Tri-*O*-acetyl-1-(*N*'-dodecylthioureido)-5*N*,6*O*-oxomethylidene-1-deoxynojirimycin (3).** To a stirred solution of the isothiocyanate derivative **2** (372 mg, 1.00 mmol) in anhydrous DCM (28 mL), *n*-dodecylamine (185 mg, 1.00 mmol) was added and the reaction mixture was stirred for 15 min at RT. The solvent was removed under reduced pressure and the resulting residue was purified by column chromatography (1:2 EtOAc-cyclohexane) to afford **3**. Yield: 490 mg (88%). $R_f$ 0.46 (1:1 EtOAc-cyclohexane). $[\alpha]_D$ +65.3 (*c* 1.1 in DCM). $^1$H NMR (300 MHz, $CDCl_3$) δ 7.43 (bs, 1 H, NH), 6.40 (d, 1 H, $J_{NH,1}$ = 6.0 Hz, NH), 5.67 (t, 1 H, $J_{1,2}$ = 6.0 Hz, H-1), 5.43 (t, 1 H, $J_{2,3}$ = $J_{3,4}$ = 9.5 Hz, H-3), 5.05 (dd, 1 H, H-2), 4.94 (t, 1 H, $J_{4,5}$ = 9.5 Hz, H-4), 4.52 (t, 1 H, $J_{6a,6b}$ = $J_{5,6a}$ = 9.0 Hz, H-6a), 4.36 (dd, 1 H, $J_{5,6b}$ = 7.6 Hz, H-6b), 4.03 (bq, 1 H, H-5), 3.59-3.50 (m, 2 H, NHC$H_2$), 2.13-2.06 (3 s, 9 H, MeCO), 1.68-1.54 (m, 2 H, $NHCH_2CH_2$), 1.36-1.18 (m, 18 H, $CH_2$), 0.87 (t, 3 H, $^3J_{H,H}$ = 7.0 Hz, $CH_3$). $^{13}$C NMR (75.5 MHz, $CDCl_3$) δ 181.9 (C=S), 170.0-169.3 (Me*C*O), 157.1 (CO), 72.4 (C-4), 68.3 (C-3), 68.2 (C-2), 67.6 (C-6), 58.4 (C-1), 51.8 (C-5), 47.0 ($NHCH_2$), 31.9-22.7 ($CH_2$), 20.6-20.4 (*Me*CO), 14.1 ($CH_3$). ESIMS: *m/z* 580.3 $[M + Na]^+$. Anal. Calcd for $C_{26}H_{43}N_3O_8S$: C 56.00, H 7.77, N 7.53, S 5.75. Found: C 55.67, H 7.55, N 7.21, S 5.41.

**(1*S*)-2,3,4-Tri-*O*-acetyl-1-(*N*'-dodecylcarbodiimido)-5*N*,6*O*-oxomethylidene-1-deoxynojirimycin (4).** To a stirred solution of the α-glycosyl thiourea **3** (490 mg, 0.88 mmol) in DCM-$H_2O$ (1:1, 21 mL), mercuric oxide (HgO) (572 mg, 2.64 mmol) was added, and the reaction mixture was stirred at RT for 1 h. Then, DCM (20 mL) was added and the organic layer was separated, dried ($MgSO_4$), filtered through a pad of Celite and concentrated under reduced pressure. The resulting residue was purified by column chromatography (1:1 EtOAc-cyclohexane) to afford **4**. Yield: 423 mg (92%). $R_f$ 0.33 (1:1 EtOAc-cyclohexane). $[\alpha]_D$ +52.0 (*c* 1.0 in DCM). $^1$H NMR (300 MHz, $CDCl_3$) δ 5.63 (d, 1 H, $J_{1,2}$ = 4.2 Hz, H-1), 5.43 (t, 1 H, $J_{2,3}$ = $J_{3,4}$ = 10.0 Hz, H-3), 4.92 (dd, 1 H, H-2), 4.88 (t, 1 H, $J_{4,5}$ = 10.0 Hz, H-4), 4.34 (dd, 1 H, $J_{6a,6b}$ = 9.0 Hz, $J_{5,6a}$ = 8.1 Hz, H-6a), 4.18 (t, 1 H, $J_{5,6b}$ = 9.0 Hz, H-6b), 4.09-3.92 (m, 1 H, H-5), 3.30-3.13 (m, 2 H, $NCH_2$), 2.03-1.97 (3 s, 9 H, MeCO), 1.59-1.46 (m, 2 H, $NCH_2CH_2$), 1.30-1.15 (m, 18 H, $CH_2$), 0.81 (t, 3 H, $^3J_{H,H}$ = 7.0 Hz, $CH_3$). $^{13}$C NMR (75.5 MHz, $CDCl_3$) δ 169.9-169.3 (Me*C*O), 154.9 (CO), 136.8 (N=C=N), 72.1 (C-4), 70.6 (C-2), 69.1 (C-3), 66.5 (C-6), 62.8 (C-1), 51.8 (C-5), 46.2 ($NCH_2$), 31.7-22.5 ($CH_2$), 20.3 (*Me*CO), 13.9 ($CH_3$). ESIMS: *m/z* 546.4 $[M + Na]^+$. HRFABMS Calcd for $C_{26}H_{41}N_3O_8SNa$ $[M + Na]^+$ 546.2786, found 546.2765.

**(1*S*)-2,3,4-Tri-*O*-acetyl-1-(*N*'-dodecylselenoureido)-5*N*,6*O*-oxomethylidene-1-deoxynojirimycin (5).** To a stirred solution of the α-dodecylcarbodiimide **4** (96 mg, 0.18 mmol) in dry tetrahydrofuran (THF) (1 mL) under Ar atmosphere, 1 N dry hydrogen chloride solution in diethyl ether (0.18 mL) was added and stirred at RT for 4 h. Then, a dry THF solution (9 mL) of LiAlHSeH (0.92 mmol) prepared *in situ*[2] was added at 0 ºC to the previous mixture. The reaction mixture was stirred for 90 min, diluted with diethyl ether (50 mL), washed with brine (10 mL), dried ($MgSO_4$), filtered and concentrated under reduced pressure. The resulting residue was purified by column chromatography

---

[2] a) H. Ishihara, M. Koketsu, Y. Fukuta, F. Nada, *J. Am. Chem. Soc*. **2001**, *123*, 8408; b) M. Koketsu, N. Takakura, H. Ishihara, *Synth. Commun*. **2002**, *32,* 3075.
To a solution of selenium powder (72 mg, 0.92 mmol) in dry THF (9 mL) under argon atmosphere, lithium aluminium hydride (35 mg, 0.92 mmol) was added at 0 ºC and the reaction mixture was stirred for 30 min, ready to use without concentration.

(1:3 EtOAc-cyclohexane) to afford **5**. Yield: 51 mg (47%), (77% considering the recovered carbodiimide **4**). $R_f$ 0.47 (1:1 EtOAc-cyclohexane). $[\alpha]_D$ +55.0 (*c* 1.3 in DCM). $^1$H NMR (500 MHz, $CDCl_3$) δ 7.75 (t, 1 H, $J_{NH,CH_2}$ = 4.8 Hz, NH), 6.83 (d, 1 H, $J_{NH,1}$ = 6.2 Hz, NH), 5.61 (t, 1 H, $J_{1,2}$ = 6.2 Hz, H-1), 5.45 (dd, 1 H, $J_{2,3}$ = $J_{3,4}$ = 9.5 Hz, H-3), 5.05 (dd, 1 H, H-2), 4.94 (t, 1 H, $J_{4,5}$ = 9.2 Hz, H-4), 4.51 (t, 1 H, $J_{6a,6b}$ = $J_{5,6a}$ = 9.0 Hz, H-6a), 4.35 (dd, 1 H, $J_{5,6b}$ = 7.6 Hz, H-6b), 4.02 (bq, 1 H, H-5), 3.63-3.56 (m, 2 H, NHC*H*$_2$), 2.12-2.04 (3 s, 9 H, MeCO), 1.68-1.54 (m, 2 H, $NHCH_2CH_2$), 1.36-1.16 (m, 18 H, $CH_2$), 0.85 (t, 3 H, $^3J_{H,H}$ = 7.0 Hz, $CH_3$). $^{13}$C NMR (125.7 MHz, $CDCl_3$) δ 180.7 (C=Se), 169.9-169.2 (Me*CO*), 157.2 (CO), 72.4 (C-4), 68.2 (C-3), 68.0 (C-2), 67.7 (C-6), 58.5 (C-1), 51.9 (C-5), 50.1 ($NHCH_2$), 31.9-22.7 ($CH_2$), 20.6-20.5 (*Me*CO), 14.1 ($CH_3$). ESIMS: *m/z* 628.2 $[M + Na]^+$. Anal. Calcd for $C_{26}H_{43}N_3O_8Se$: C 51.65, H 7.17, N 6.95. Found: C 51.40, H 6.89, N 6.63.

**(1*S*)-(*N*'-Dodecylselenoureido)-5*N*,6*O*-oxomethylidene-1-deoxynojirimycin (DSeU).** To a stirred solution of **5** (80 mg, 0.13 mmol) in MeOH (5 mL), NaOMe (1 M in MeOH) (39 mL, 0.04 mmol) was added and the reaction mixture was stirred at RT for 60 min. Neutralization with solid $CO_2$, evaporation of the solvent under reduced pressure and purification by column chromatography (10:1 DCM-MeOH) afforded **DSeU**. Yield: 51 mg (82%). $R_f$ 0.67 (9:1 DCM-MeOH). $[\alpha]_D$ -11.2 (*c* 1.0 in DMSO). $^1$H NMR (300 MHz, $(CD_3)_2SO$) δ 8.03 (t, 1 H, $J_{NH,CH_2}$ = 4.7 Hz, NH), 7.94 (d, 1 H, $J_{NH,1}$ = 7.2 Hz, NH), 5.95 (bs, 1 H, H-1), 5.57 (d, 1 H, $J_{OH,4}$ = 5.0 Hz, OH), 5.50 (d, 1 H, $J_{OH,2}$ = 3.3 Hz, OH), 5.16 (d, 1 H, $J_{OH,3}$ = 3.9 Hz, OH), 4.32 (t, 1 H, $J_{6a,6b}$ = $J_{5,6a}$ = 8.1 Hz, H-6a), 4.14 (dd, 1 H, $J_{5,6b}$ = 3.0 Hz, H-6b), 3.55-3.31 (m, 5 H, H-2, H-3, H-5, NHC*H*$_2$), 3.12 (td, 1 H, $J_{3,4}$ = $J_{4,5}$ = 9.0 Hz, H-4), 1.55-1.41 (m, 2 H, $NHCH_2CH_2$), 1.35-1.15 (m, 18 H, $CH_2$), 0.85 (t, 3 H, $^3J_{H,H}$ = 7.0 Hz, $CH_3$). $^{13}$C NMR (75.5 MHz, $(CD_3)_2SO$) δ 183.3 (C=Se), 155.1 (CO), 72.9-72.8 (C-4, C-3), 69.8 (C-2), 65.4 (C-6), 64.4 (C-1), 53.7 (C-5), 46.5 ($NHCH_2$), 31.3-22.1 ($CH_2$), 13.9 ($CH_3$). ESIMS: *m/z* 478.1 $[M - H]^-$. Anal. Calcd for $C_{20}H_{37}N_3O_5Se$: C 50.20, H 7.79, N 8.78. Found: C 49.91, H 7.55, N 8.66.

## S2.3. $^{1}H$ and $^{13}C$ NMR spectra

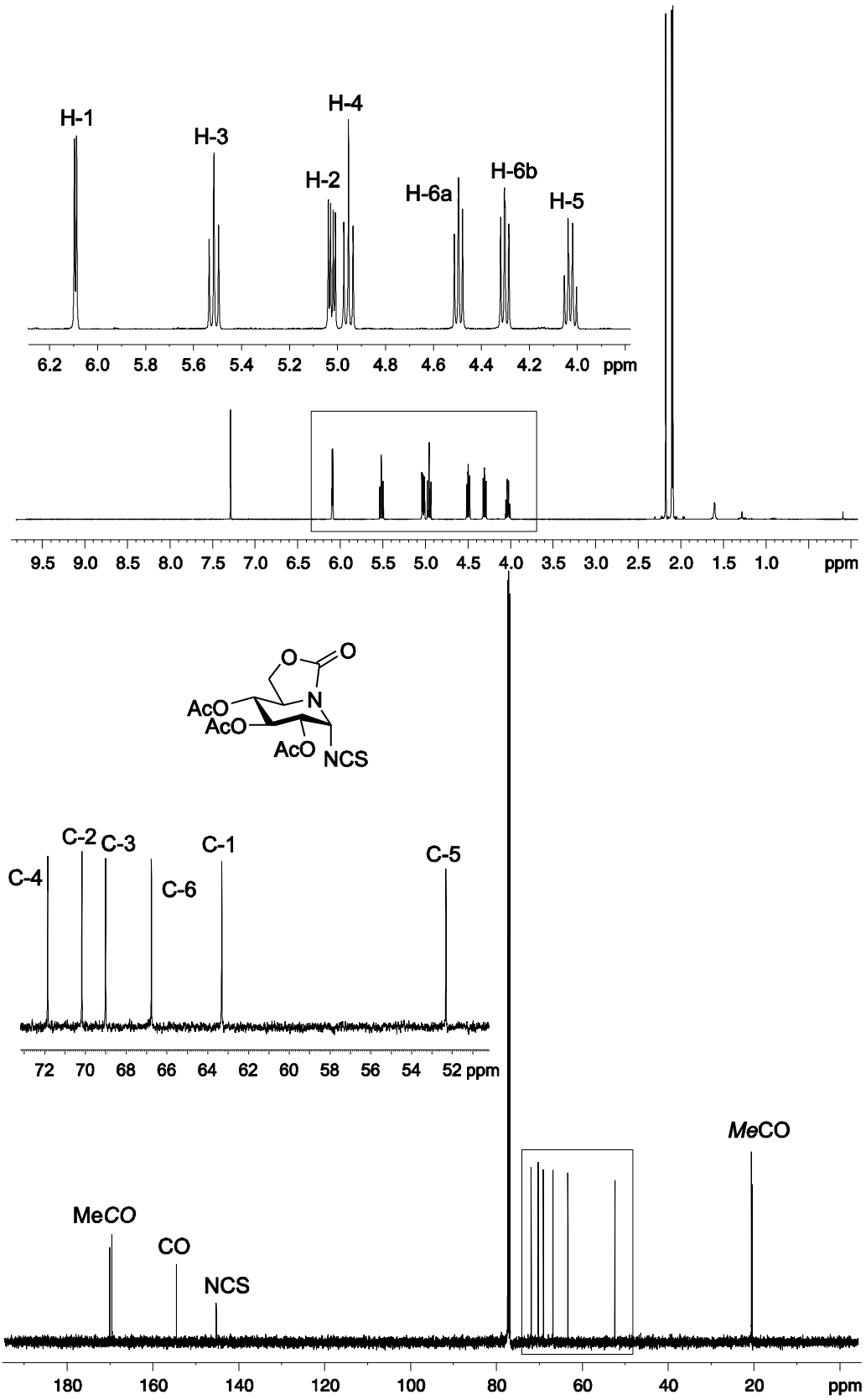


**Figure S2.** $^{1}H$ and $^{13}C$ NMR spectra (500 MHz and 125.7 MHz, $CDCl_3$) of **2**.

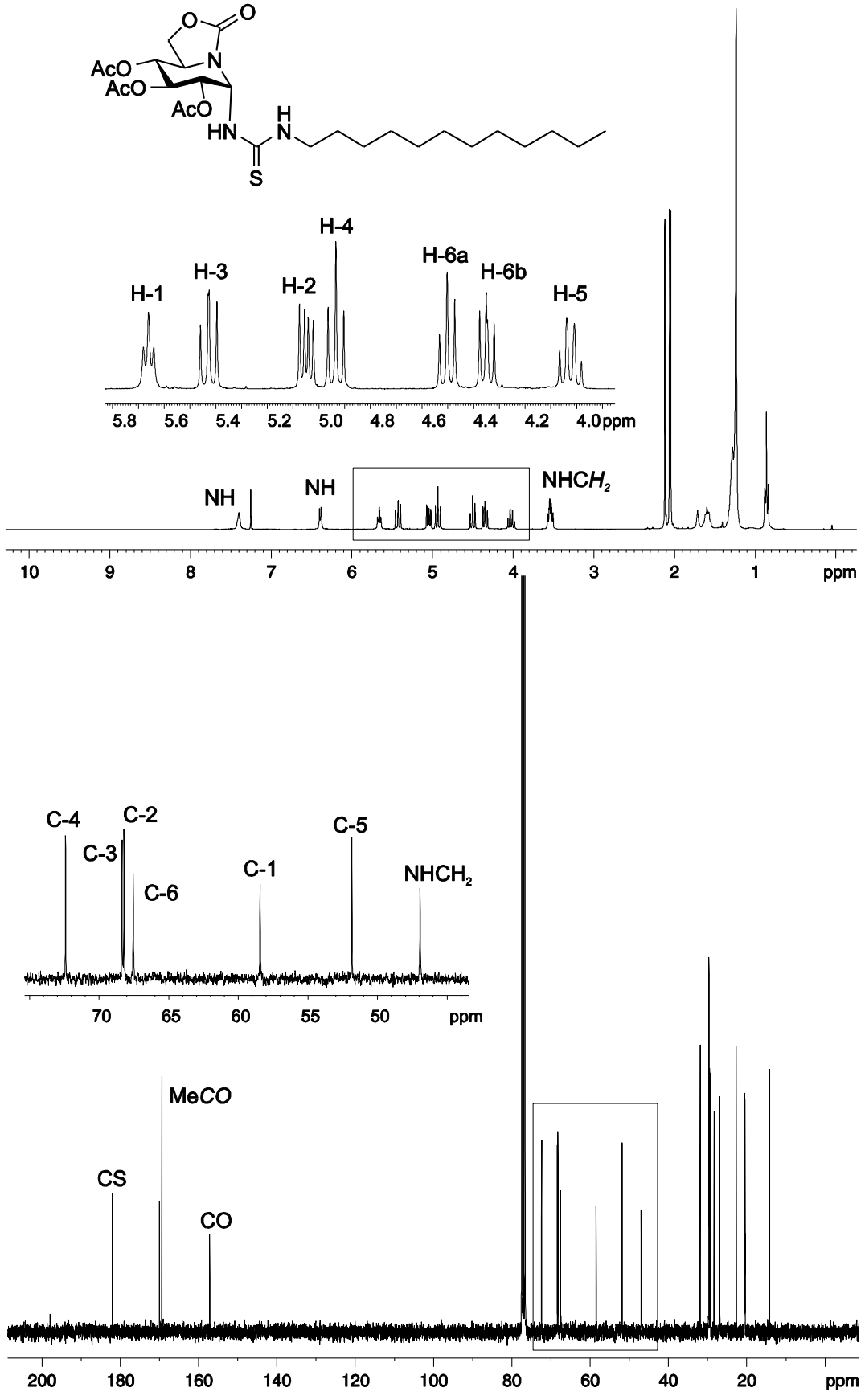


**Figure S3.** $^{1}H$ and $^{13}C$ NMR spectra (300 MHz and 75.5 MHz, $CDCl_3$) of **3**.

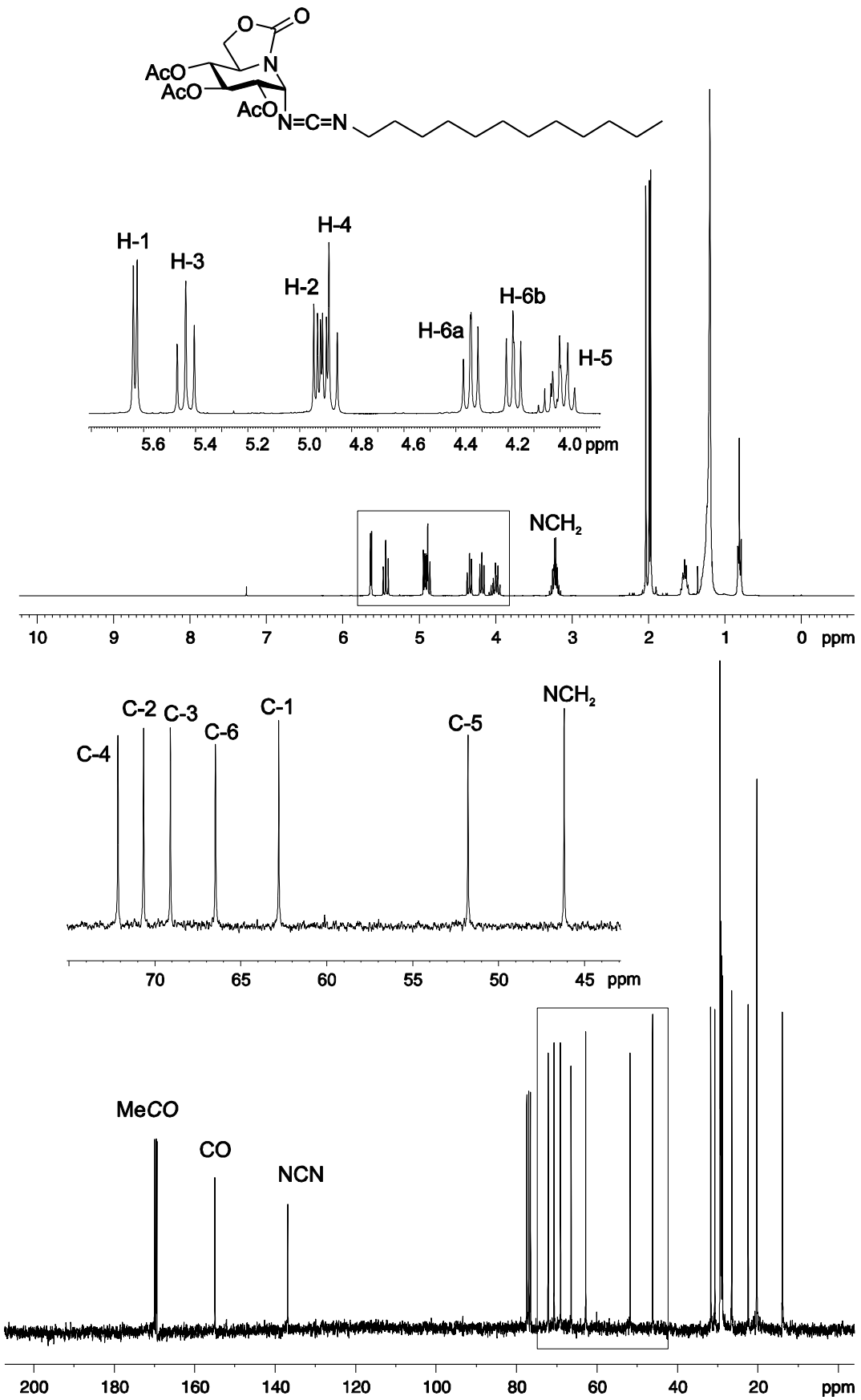


**Figure S4.** $^{1}H$ and $^{13}C$ NMR spectra (300 MHz and 75.5 MHz, $CDCl_3$) of **4**.

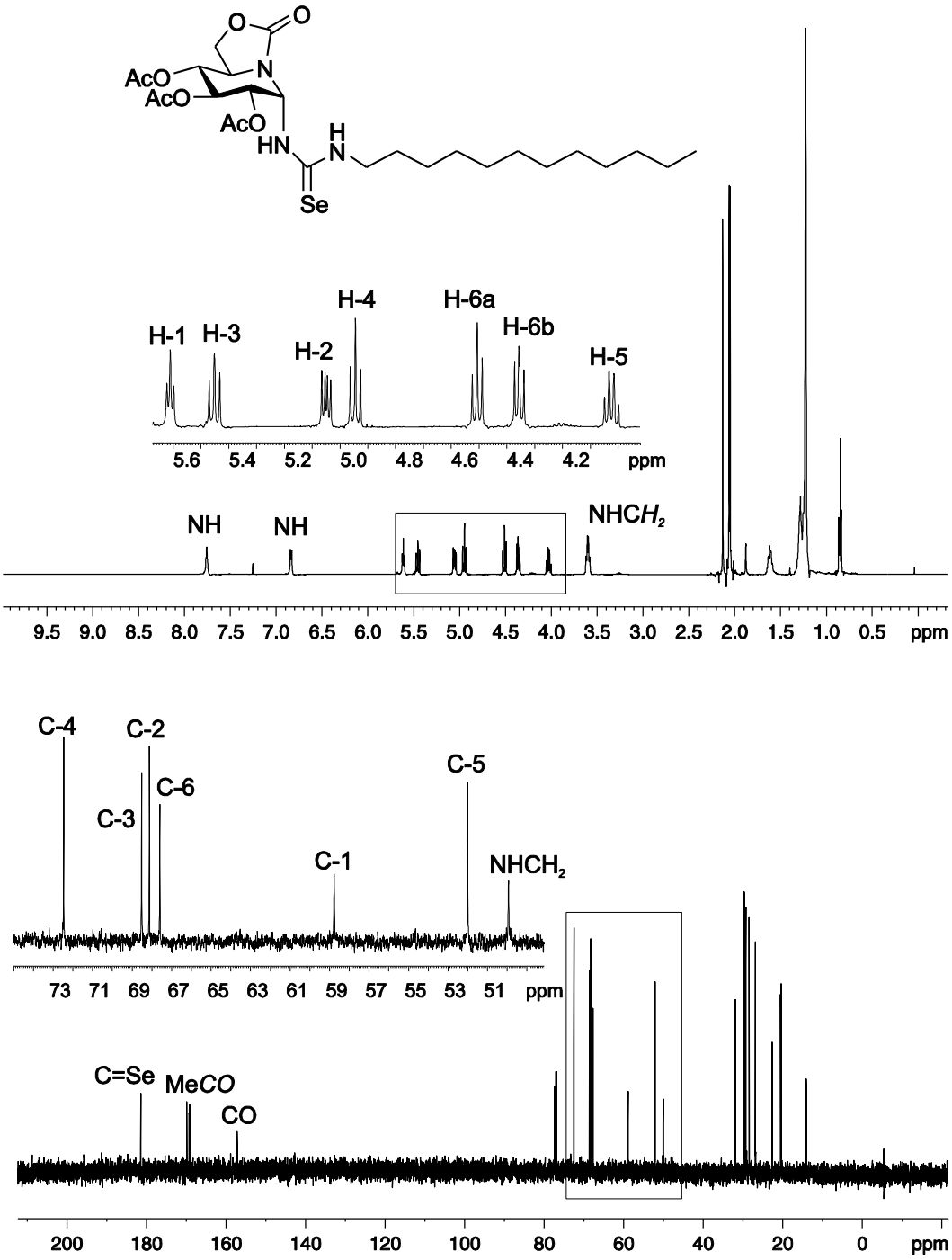


**Figure S5.** $^{1}H$ and $^{13}C$ NMR spectra (500 MHz and 125.7 MHz, $CDCl_3$) of **5**.

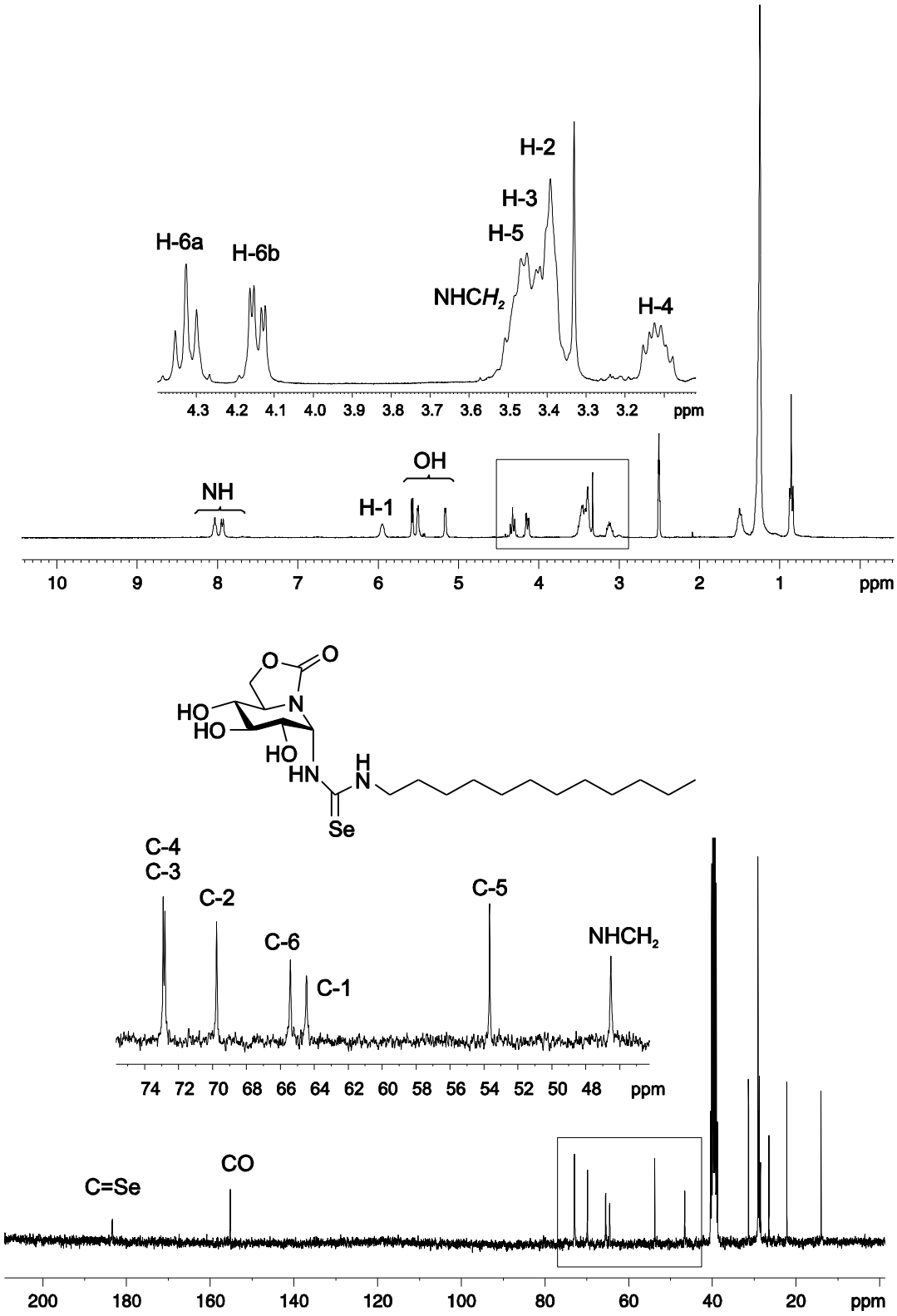


**Figure S6.** $^{1}H$ and $^{13}C$ NMR spectra (300 MHz and 75.5 MHz, $(CD_3)_2SO$) of **DSeU**.

## S3. Preparation of ZIF-based nanostructures containing (DSeU@ZIF8)

### S3.1. Optimized synthetic procedure for DSeU@ZIF8 nanoparticles

In a typical procedure, an aqueous solution of 2-methylimidazole (HmIM; 3mL, 1.3 M) was placed in a 12-mL glass vial with a magnetic stir bar, followed by the addition of an aqueous solution of zinc nitrate (($Zn(NO_3)_2$; 3 mL, 0.025 M) under continuous stirring (350 rpm) and at room temperature (RT). After that, a methanolic solution of DSeU (0.6 mL, 10 mM) was added, the mixture was stirred for 2 min, and left then undisturbed at RT for 2 h. The mixture slowly turned turbid, indicative of the formation of the particles. The resulting DSeU@ZIF8 particles were purified by centrifugation (13000 rpm, 15 min), followed by three times of washing using methanol (MeOH) and finally redispersed in MeOH at a concentration of 10 mg/mL, and store in the fridge (4 °C) until use.

Rhodamine B-loaded DSeU@ZIF8 particles (RhB@DSeU@ZIF8): To easily visualize the internalization of DSeU@ZIF8 particles in cells, these particles were loaded with a fluorescent dye (rhodamine B, RhB). For that, the as-synthetized DSeU@ZIF8 particles as dispersed in MeOH (200 µL, 10 mg/mL) were mixed with a solution of RhB in MeOH (100 µL, 1 mg/mL). The mixture was incubated overnight at RT and then the excess of the dye was removed by centrifugation. Next, the RhB@DSeU@ZIF8 particles were washed twice with MeOH, redispersed in MeOH at a concentration of 10 mg/mL, and store in the fridge until use. The loading amount of RhB was calculated by UV-vis spectroscopy at 550 nm (subtracting the RhB amount in the supernatants from the total amount in the initial solution), and it was found to be 21 mg RhB per g DSeU@ZIF8 particles.

### S3.2. Determination of EE% and LC%

The amount of DSeU encapsulated on the ZIF particles was quantified indirectly, by measuring by HPLC analyses the DSeU remaining in the supernatant after centrifugation and washing steps of the DSeU@ZIF8 particles. The calibration curve was obtained by using standards solutions (with known concentrations) of DSeU and using a previously optimized method for HPLC-MS analysis. The encapsulation efficiency (EE%) was calculated by the following equation:

$$\text{EE}\ (\%) = \frac{\mu mol\ DSeU_{\text{encapsulated}}}{\mu mol\ DSeU_{\text{added}}} \times 100 = \frac{\mu mol\ DSeU_{\text{added}} - \mu mol\ DSeU_{\text{non-encapsulated}}}{\mu mol\ DSeU_{\text{added}}} \times 100$$

For determining the loading capacity (LC), 50 µL of the DSeU@ZIF8 stock solution (10 mg/mL) were incubated with 20 µL of HCl to destroy (dissolve) the particles, and the resulting mixture was analysed by HPLC-MS. In this way the amount of DSeU encapsulated per gram of particles was calculated using the following equation:

$$\text{LC}\ (wt\%) = \frac{mg\ DSeU_{\text{encapsulated}}}{mg\ DSeU@ZIF8}\ x\ 100$$

Under the final optimized experimental conditions, the EE% and LC% were found to be 97 % and 5.8 wt%, respectively.

## S3.3. Influence of experimental synthetic conditions

The ratio of precursors, reaction media and growth time were optimized in order to simultaneously achieve: i) high EE%, ii) particles smaller than 100 nm; and iii) control on the number of micelles per nanoparticle (MIC/NP, ideally one DSeU micelle per ZIF particle). During the optimization process, the particle size (hydrodynamic diameter, $d_h$) and polydispersity (PdI) of the samples were monitored by DLS, while the morphology and micelles per particle were determined by TEM. Results obtained under different studied conditions are presented in Table S1 and Figures S7 and S8, showing that the amount of DSeU and the media composition influenced strongly the synthesis process. The influence of the time on the synthesis was studied ranging from 30 min to 18 h, monitoring the evolution of the particle size over time by DLS. The kinetic of the DSeU@ZIF8 formation was quite fast, observing the appearance of turbidity just 5 min after mixing the precursors. In contrast, control ZIF8 particles presented a slower kinetic, without visual observation of nucleation until after around 50 min. Despite this fast nucleation of DSeU@ZIF8, the further growth of the particles was limited, reaching the maximum size after 2 h and not observing size changes for longer times. Finally, the order of addition of the precursors using the optimized condition (A3c in Table S1) was also investigated. To do this, first the methanolic solution of DSeU was added to the aqueous solution of $Zn(NO_3)_2$ with stirring, observing the formation of a precipitate, most likely due to the formation of Zn-DSeU complexes or the destabilization of the DSeU micelles with the consequent insolubilization of the DSeU molecules in that medium ($H_2O$:MeOH, 5:1). The HmIM solution was then added to the above mixture, stirred for 2 min and left undisturbed at RT for 2 h. As shown in Figure S7F, no control over the synthesis was achieved under this condition, clearly indicating that the order of addition of the precursors was also critical.

**Table S1**. Optimization data for the synthesis of DSeU@ZIF8 particles. The selected optimal conditions are shades in red.

| Sample | HmIM (M) | $Zn^{+2}$ (mM) | DSeU (mM) | Media $H_2O$:MeOH | Time (h) | EE (%) | $d_h$ ± SD (nm) | MIC/NP |
|---|---|---|---|---|---|---|---|---|
| A1 | 0.59 | 11.4 | 0.18 | 10:1 | 6 | 8.7 | 42 ± 3.9 | 0 |
| A2 | 0.59 | 11.4 | 0.45 | 10:1 | 6 | 71 | 68 ± 3.7 | 0/1 |
| A3 | 0.59 | 11.4 | 0.91 | 10:1 | 6 | 98 | 75 ± 2.9 | 1 |
| A4 | 0.59 | 11.4 | 1.82 | 10:1 | 6 | 98 | 107 ± 4.5 | n.c.* |
| A3a | 0.59 | 11.4 | 0.91 | 10:1 | 0.5 | 96 | 48 ± 3.0 | 1 |
| A3b | 0.59 | 11.4 | 0.91 | 10:1 | 1 | 97 | 63 ± 2.6 | 1 |
| A3c | 0.59 | 11.4 | 0.91 | 10:1 | 2 | 97 | 75 ± 2.9 | 1 |
| A3d | 0.59 | 11.4 | 0.91 | 10:1 | 6 | 97 | 78 ± 3.1 | 1 |
| A3e | 0.59 | 11.4 | 0.91 | 10:1 | 18 | 97 | 80 ± 4.2 | 1 |
| A5 | 0.59 | 11.4 | 0.91 | 1:1 | 2 | 21 | 185 ± 3.1 | 0 |

*n.c.= no control on the number of micelles per nanoparticle

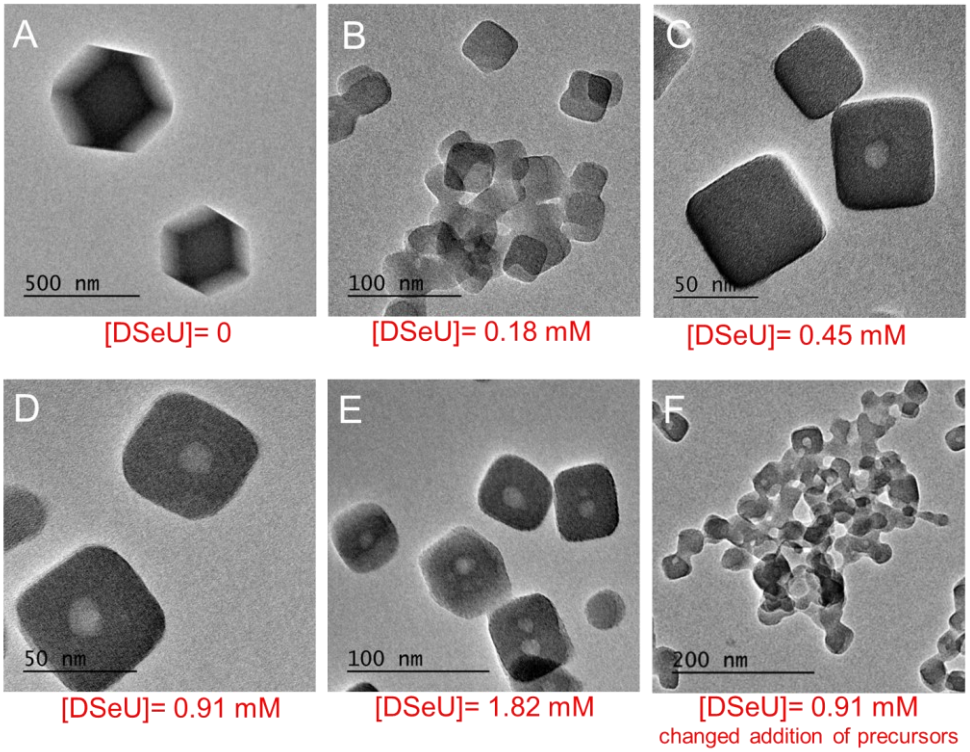


**Figure S7.** Representative TEM images of DSeU@ZIF8 particles prepared with different amounts of DSeU but maintaining constant the other parameters: (A) 0, (B) 0.18 mM (1.2 μmol), (C) 0.45 mM (3.0 μmol), (D) 0.91 mM (6.0 μmol), and (E) 1.82 mM (12 μmol). (F) Particles prepared with the optimized amount of DSeU (0.91 mM) but changing the order of addition of the precursor solutions as indicated in the text.

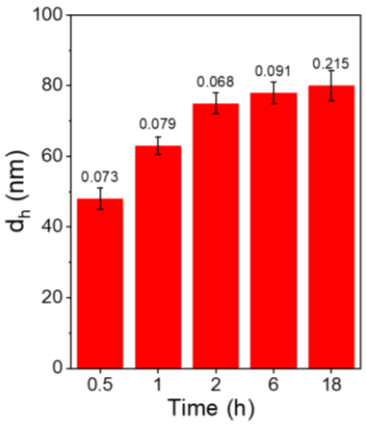


| Time (h) | $d_h$ ± SD (nm) |
|---|---|
| 0.5 | 48 ± 3.0 |
| 1 | 63 ± 2.5 |
| 2 | 75 ± 2.9 |
| 6 | 78 ± 3.1 |
| 18 | 80 ± 4.2 |

**Figure S8.** Hydrodynamic size ($d_h$, mean ± SD) of the DSeU@ZIF8 particles dispersed in MeOH as a function of the synthesis time, as determined by DLS. Polydispersity index (PDI) values are given on columns.

## S3.4. Synthesis of pristine ZIF8 particles as control

Two types of ZIF8 control particles, that is without incorporating the DSeU, were prepared. For ZIF8 control 1 (ZIF8/Cnt1), the synthesis was performed as described above but adding 0.6 mL of MeOH instead of the methanolic solution of DSeU. Due to the absence of a modulator agent during the synthesis, these particles (Figure S9A) were much bigger than the designed DSeU@ZIF8 particles. In order to obtain control ZIF8 particles having a size (< 100 nm) similar to those that DSeU@ZIF8 particles, ZIF8 control 2 (ZIF8/Cnt2) were prepared using the surfactant cetyltrimethylammonium bromide (CTAB) as size-controlling agent; Figure S9B. Briefly, an aqueous solution of HmIM (3mL, 1.3 M) was placed in a 12-mL glass vial with a magnetic stir bar, followed by the addition of an aqueous solution of $Zn(NO_3)_2$ (3 mL, 0.025 M) under continuous stirring (350 rpm) at RT, and immediately after an aqueous solution of CTAB (3 mL, $2.0\times10^{-3}$ M) was added. The mixture was stirred for 2 min, and left then undisturbed for 2 h. In both cases, the purification step was the same as that performed with DSeU@ZIF8 particles, and ZIF8/Cnt1 and ZIF8/Cnt2 particles were finally redispersed in MeOH at a concentration of 10 mg/mL and store at 4 °C until use.

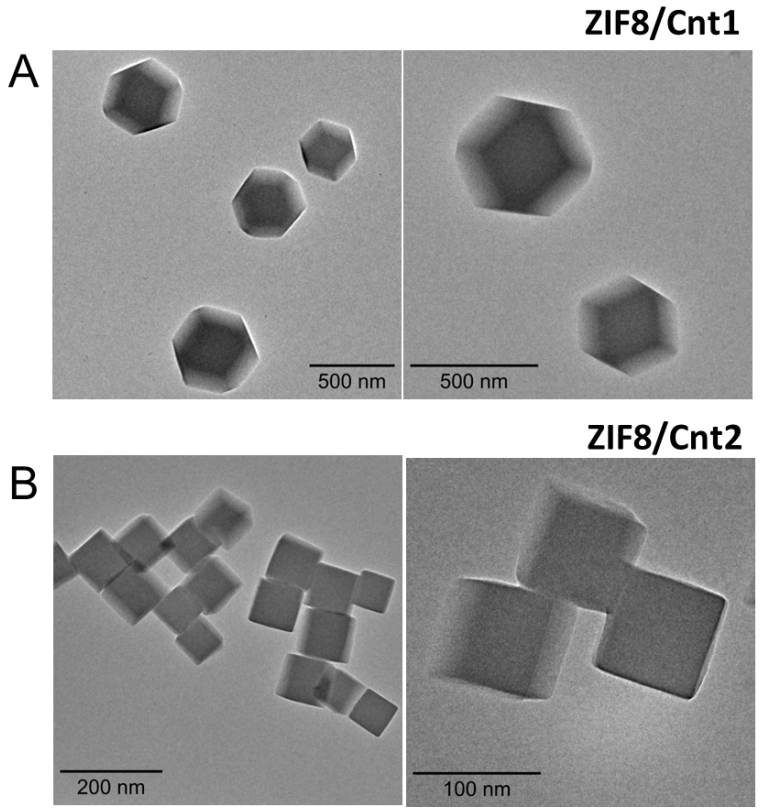


**Figure S9.** Representative TEM images of two types of prepared ZIF8 control particles, (A) ZIF8/Cnt1 and (B) ZIF8/Cnt2. The sample ZIF8/Cnt2 was selected as control particles and denoted from now on as ZIF8.

## S4. Morphological/Structural characterization of DeU@ZIF8 particles

### S4.1. Supporting structural characterization data

The morphology, crystalline structure, colloidal stability in solution and textural properties of the as-prepared DSeU@ZIF8 particles, as well as that of the control ZIF8 particles were investigated by diverse characterization techniques, such as TEM, SEM-EDX, DLS, PXRD, and physisorption analysis. Additional figures and tables (not included in main manuscript) related to the structural properties of the particles are provided below.

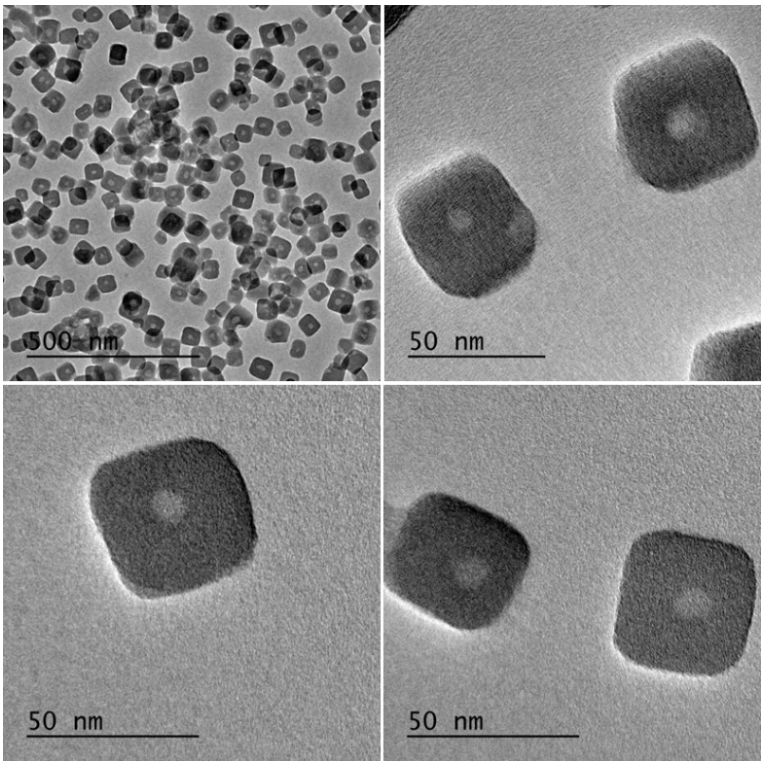


**Figure S10.** Representative TEM images of DSeU@ZIF8 particles prepared under the optimized conditions.

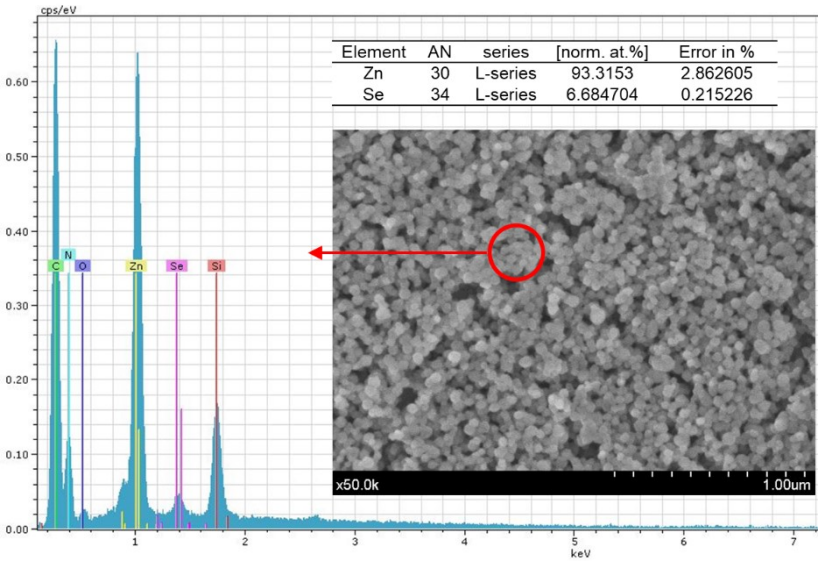


**Figure S11**. SEM-EDX analysis of the DSeU@ZIF8 particles, showing the presence of the expected elements with a Se/Zn ratio = 0.072.

$^{1}$H NMR was used to confirm the successful encapsulation of the DSeU inside the ZIF structure. DSeU@ZIF8 particles (dispersed in $CD_3OD$) were dissolved by adding diluted $H_2SO_4$ and $^{1}$HNMR spectrum of these mixtures was compared with that of the DSeU@ZIF8 particles (before dissolution) and the free DSeU (before encapsulation), Figure S12.

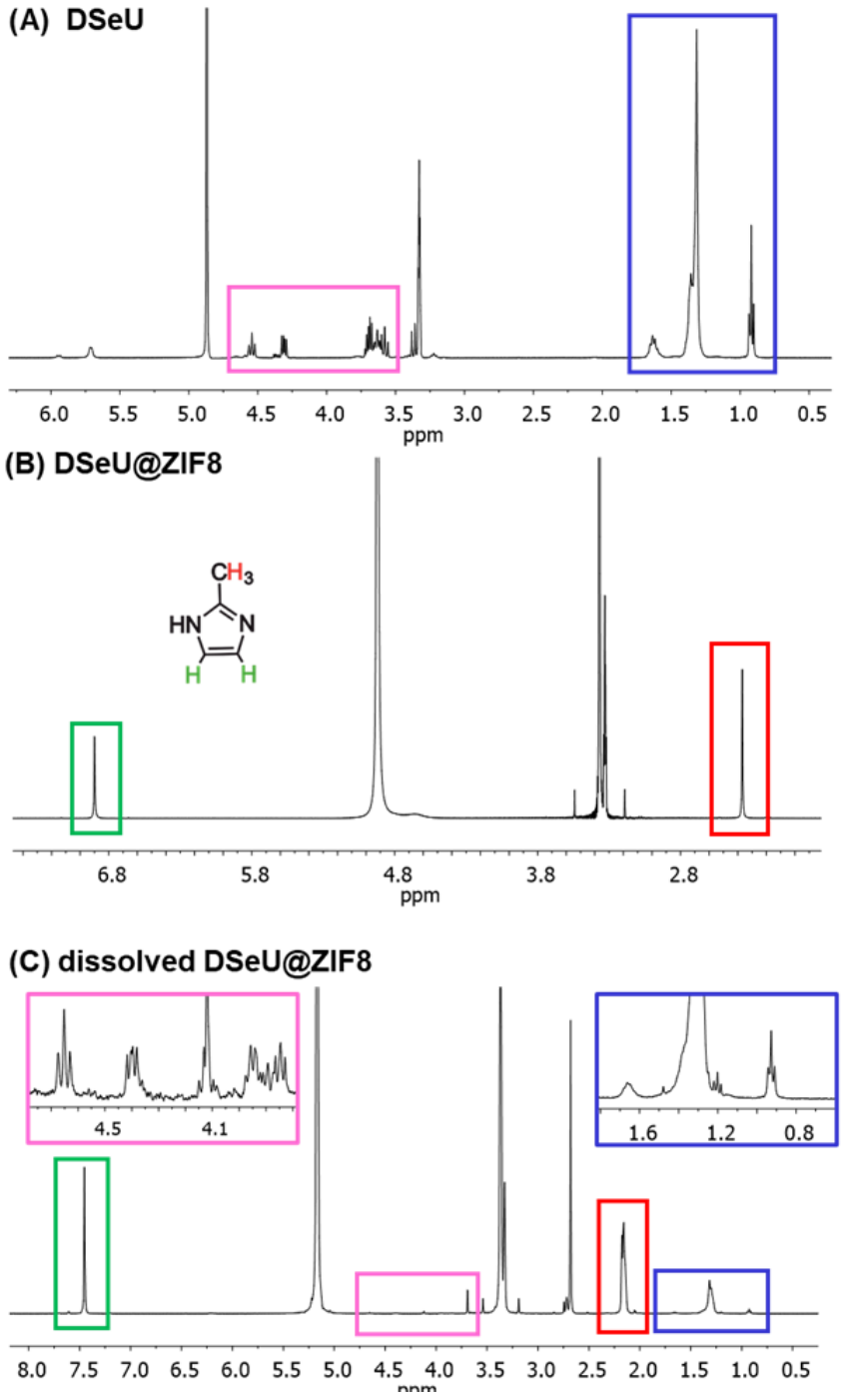


**Figure S12**. $^{1}$H NMR spectra recorded at 400 MHz of (A) free DSeU in $CD_3OD$; (B) DSeU@ZIF8 particles dispersed in $CD_3OD$; and (C) DSeU@ZIF8 dissolved in $CD_3OD$.

**Table S2**. Hydrodynamic diameters $d_h$ (mean ± standard deviation SD) in either MeOH or Milli-Q water and ζ-potential in Milli-Q water of DSeU@ZIF8 and control ZIF8 particles as derived from DLS number distributions and LDA measurements, respectively.

| | MeOH | | Water | | |
|---|---|---|---|---|---|
| **Sample** | **$d_h$ ± SD (nm)** | **PDI** | **$d_h$ ± SD (nm)** | **PDI** | **ζ ± SD (mV)** |
| ZIF8 | 103 ± 3.6 | 0.112 | 109.7 ± 3.5 | 0.111 | 11.2 ± 1.3 |
| DSeU@ZIF8 | 75.1 ± 1.1 | 0.175 | 79.1 ± 3.7 | 0.191 | 11.9 ± 1.4 |

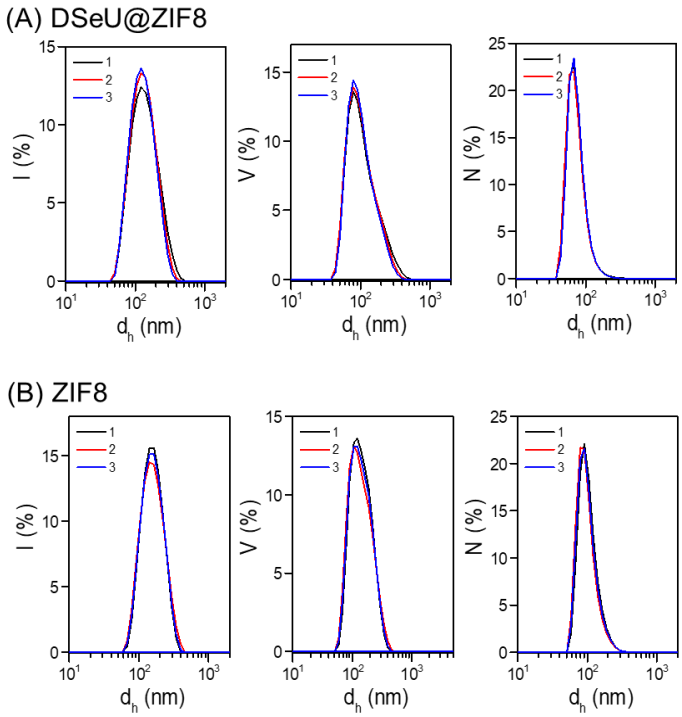


**Figure S13.** DLS intensity (I), volume (V), and number (N) distributions of the hydrodynamic diameter $d_h$ of (A) DSeU@ZIF8 and (B) control ZIF8 particles as dispersed in MeOH.

Taking into account that the DSeU fraction in the DSeU@ZIF8 particles accounts for about 5.8 wt % as determined by HPLC, their textural data were corrected considering exclusively the ZIF weight (Table S4).

**Table S3**. Textural properties of DSeU@ZIF8 and control ZIF8 particles.

| **Sample** | **$S_{BET}$ ($m^2/g$)** | **$S_{micro}$ ($m^2/g$)** | **$V_{micro}$ ($cm^3/g$)** | **$S_{BET}$* ($m^2/g$)** | **$S_{micro}$* ($m^2/g$)** | **$V_{micro}$* ($cm^3/g$)** |
|---|---|---|---|---|---|---|
| ZIF8 | 1243 | 1213 | 0.565 | — | — | — |
| DSeU@ZIF8 | 1194 | 946 | 0.435 | 1267 | 1004 | 0.462 |

Total surface area calculated by BET equation ($S_{BET}$); micropore area ($S_{micro}$) and micropore volume ($V_{micro}$) were calculated by t-plot method.

*Corrected considering exclusively the ZIF8 weight.

## S4.2. Colloidal and chemical stability of particles

DLS was used to study the colloidal stability of the as-prepared DSeU@ZIF8 particles in different media, Fig. 2C and Table S4.

**Table S4**. Hydrodynamic diameters $d_h$ (mean ± SD) at different time points as derived from DLS number distributions of the DSeU@ZIF8 and control ZIF8 particles dispersed in either Milli-Q water (pH ~6.0) or acid medium (acetate buffer solution, pH=4.5). Data correspond to the raw data shown in Figure 2C of the main text.

| | **$d_h$ ± SD (nm)** | | | |
|---|---|---|---|---|
| | **Milli-Q water** | | **Acetate buffer solution** | |
| **Time (h)** | **DSeU@ZIF8** | **ZIF8** | **DSeU@ZIF8** | **ZIF8** |
| 0 | 79.1 ± 3.7 | 109.9 ± 3.5 | 75.2 ± 4.0 | 110.3 ± 5.3 |
| 1 | 82.3 ± 2.2 | 110.5 ± 2.5 | 70.5 ± 4.5 | 66.5 ± 10.3 |
| 6 | 85.2 ± 2.5 | 105.0 ± 3.2 | 67.2 ± 6.3 | - |
| 24 | 80.2 ± 3.2 | 98.0 ± 4.9 | 45.2 ± 8.0 | - |
| 48 | 80.6 ± 2.5 | 96.2 ± 4.3 | - | - |
| 72 | 78.3 ± 1.9 | 87.3 ± 3.5 | - | - |
| 168 | 76.4 ± 2.4 | 65.2 ± 6.7 | - | - |

The chemical stability of DSeU@ZIF8 under acidic medium, and its comparison with the pristine ZIF8, was investigated by incubating the particles in acetate buffer solution at pH=4.5 (prepared in $D_2O$) for different times, and analyzing the supernatants (after separation of the particles by centrifugation) by $^1$H NMR (Fig. S14-15). This allowed us to determine the amount of HmIM released over time in each case, Fig. S16A, showing that ZIF8 degraded much faster than DSeU@ZIF8 particles. The total content of HmIM in the particles was determined by analysing the resulting mixture after digestion of the particles with HCl. The percentages of HmIM release over time (Fig. S16B) were calculated using the integration values from the methyl group of 2-methylimidazole (Int-$CH_3$) in each sample and applying the following equation:

$$HmIM\ release\ (\%) = \frac{Int-CH_3,\ HmIM_{released}}{Int-CH_3,\ HmIM_{total}} x\ 100$$

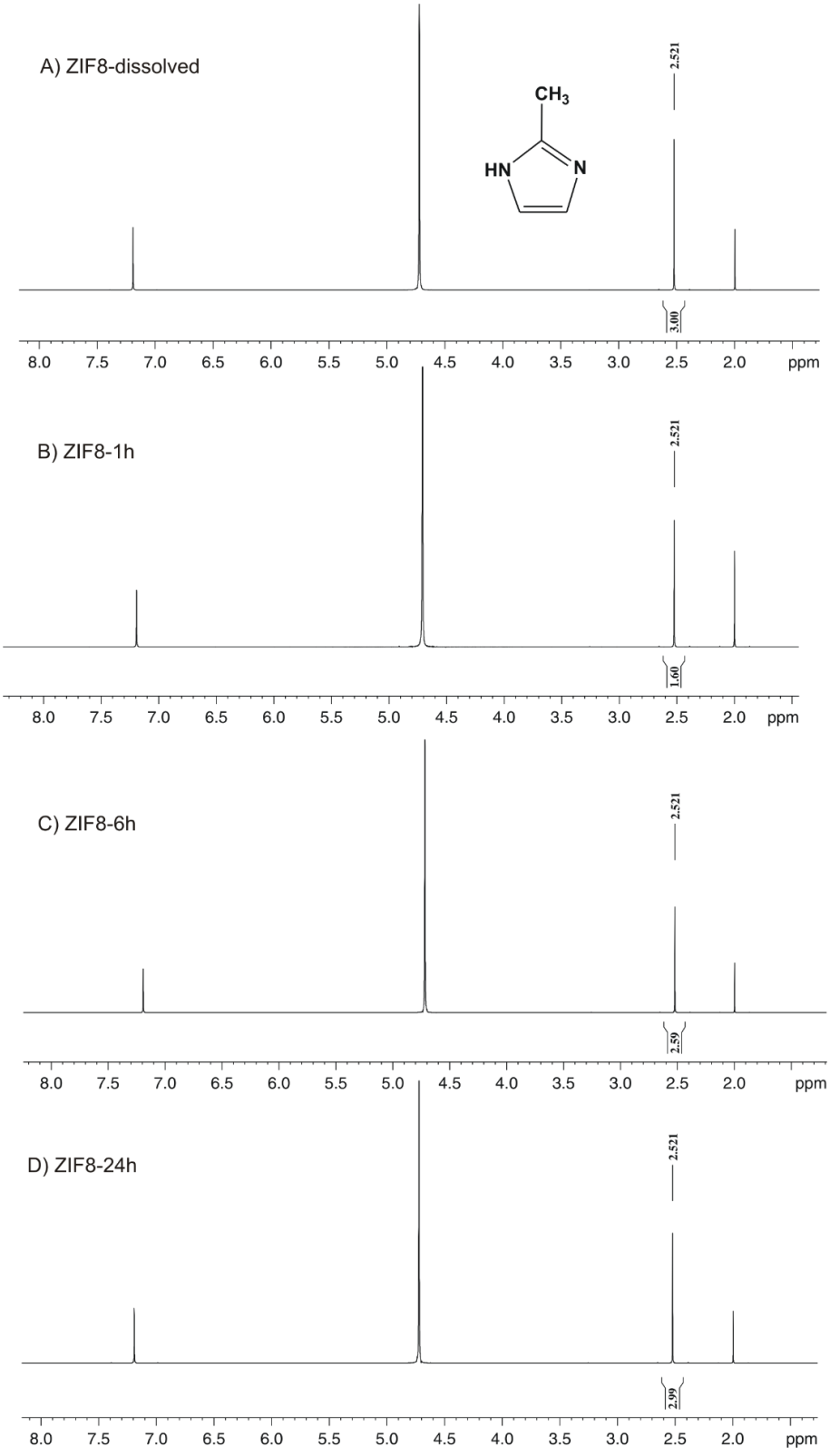


**Figure S14.** $^{1}H$ NMR spectra (500 MHz, $D_2O$) of supernatants collected after incubation of ZIF8 particles in acidic medium (acetate buffer solution at pH=4.5 prepared in $D_2O$) at different times: 1 h (B), 6 h (C), 24 h (D). The integration values from the methyl group of 2-methylimidazole released are shown for each spectrum considering 3H for the total release, that is, ZIF8-dissolved (spectrum A).

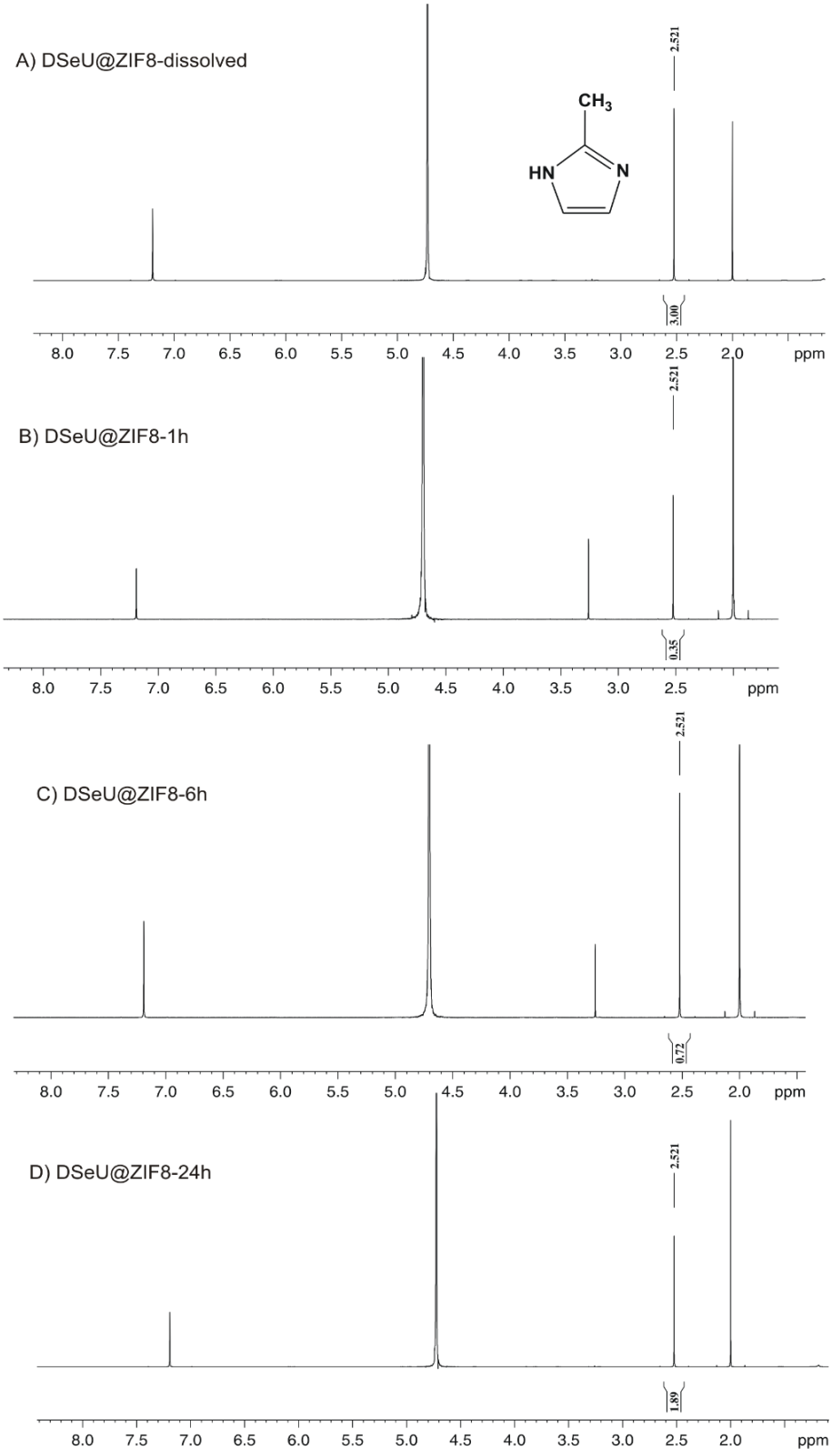


**Figure S15.** $^{1}$H NMR spectra (500 MHz, $D_2O$) of supernatants collected after incubation of DSeU@ZIF8 particles in acidic medium (acetate buffer solution at pH=4.5 prepared in $D_2O$) at different times: 1 h (B), 6 h (C), 24 h (D). The integration values from the methyl group of 2-methylimidazole released are shown for each spectrum considering 3H for the total release, that is, ZIF8-dissolved (spectrum A).

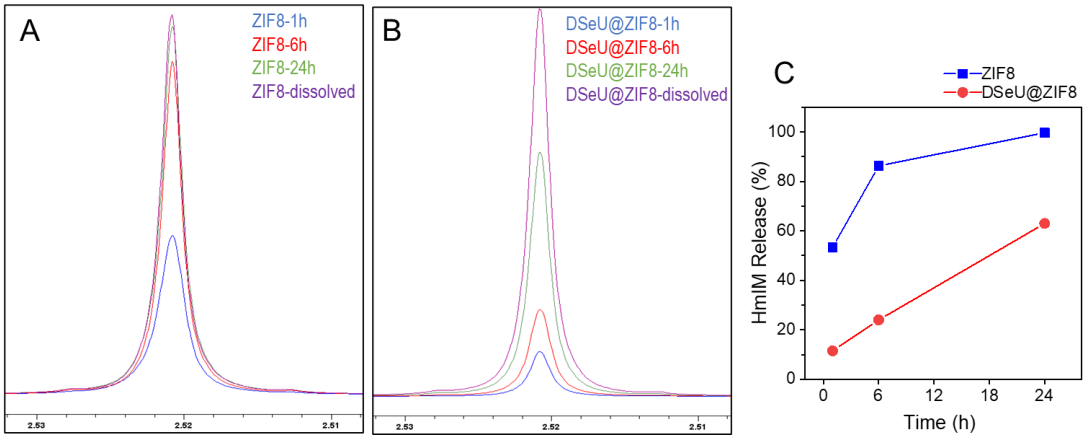


**Figure S16.** (A-B) $^{1}$H NMR signal of the methyl group (δ 2.52 ppm) from the release of 2-methylimidazole after incubation of the particles in acid medium at different times. (C) Kinetic profiles of HmIM released from the DSeU@ZIF8 and ZIF8 particles dispersed in acetate buffer solution at pH=4.5, as determined by $^{1}$H NMR quantification.

## S4.3. Release study of DSeU under different conditions

*pH effect.* DSeU release performance of the DSeU@ZIF8 at different pH environments was assessed by monitoring the amount of DSeU released over time (from 0 to 48 h) upon incubation of the particles (1 mL, 5 mg/mL) in two different pH media. Specifically, Tris-HCl buffer solution (pH=7.4, 10 mM) was used to mimic extracellular conditions, whereas acetate buffer solution (pH=4.5, 10 mM) simulated intracellular conditions (lysosomal/endosomal compartments) and also inflammatory tissues. After each incubation time of the DSeU@ZIF8 particles in each media, vials were centrifugated to separate the particles (pellets) and the supernatants (containing the DSeU released) were taken and analysed by HPLC.

*Cell medium effect*. It is well-known the instability of the ZIF8 structure in the presence of phosphate ions due to their attack to $Zn^{+2}$ (Lewis metal centers) on the surface of the particles. Since endothelial cell culture medium (ECM) contains phosphate buffers in its composition, the potential degradation of the DSeU@ZIF8 particles in this ECM could lead to unwanted extracellular release of DSeU. To investigate the ECM effect on the DSeU@ZIF8 particles, the release of DSeU over time after suspension of the particles in ECM was monitored. After each incubation time, vials were centrifugated to separate the particles (pellets) and the supernatants (containing the DSeU released) were taken and analysed by HPLC.

The amount of DSeU released at each time under the different conditions was quantified by using previously obtained calibration curve (using standards of known concentrations). The total content of DSeU in the particles was determined by analysing the resulting mixture after digestion of the particles with HCl. The percentages of DSeU release over time (shown in Figure 2F in the main text) were calculated using the following equation:

$$DSeU\ release\ (\%) = \frac{mg\ DSeU_{released}}{mg\ DSeU_{total}}\ x\ 100$$

## S5. Evaluation of the performance of DeU@ZIF8 particles in cells

### S5.1. Cell culture and compound/particle treatments

It is important to note that we selected human umbilical vein endothelial cells (HUVECs) as model cells because of their ability to closely mimic the vasculature and study endothelial cell dynamics *in vitro*. This makes them an important tool in various research fields, including inflammation, oxidative stress, infection response, and normal and tumor-associated angiogenesis.

HUVECs were obtained from Cell Systems (Clonetics, Solingen, Germany). Cells were cultured at 37 °C in 95% humidity and 5% $CO_2$ atmosphere in ECM, which consisted of endothelial basal medium (EBM) plus endothelial cell growth medium supplements (EGM, Cambrex Bioscience) and 10% (v/v) fetal bovine serum (FBS, Invitrogen). The supplemented medium is then named as complete medium. Briefly, fresh cells were seeded in T-75 culture flasks and the medium was changed every 48 h. When the cells in culture reached 80% confluence was reached, cells were detached with trypsin-EDTA solution and subcultured in completed medium in 96-well plates (opaque tissue culture treated plate, Greiner Bio-One) for 24 h prior to the addition of the compounds/nanoparticles.

Three experimental groups were studied, corresponding to cells treated with the free DSeU, ZIF8 particles or DSeU@ZIF8 particles. In addition, two control groups were used, one group of untreated cells (as negative control, Cnt-), and other group treated with $H_2O_2$ (as positive control, Cnt+). Concentrations used in experiments shown in Figure 3 of the main text ranged from 0.5 to 50 μM (expressed as the concentration of DSeU, either as free compound or encapsulated into particles), and different incubation time were also studied. Finally, the standard treatment with compound/particles for experiments shown in Figure 4 and 5 consisted on incubating cells for 24 h with either 1 μM of free DSeU, or equivalent 8.2 μg/mL for particles (this equivalent concentration was determined taking into account that the DSeU fraction in the particles was 5.8 wt%). Each time, just before the experiment, DSeU or particles were diluted in FBS-free media and shaken well to ensure equal dispersion of particles in solution.

To establish the optimal experimental conditions for the *in vitro* model of oxidative stress-injury ($H_2O_2$-induced HUVEC cells), concentration- and time- response studies were performed (Figures 4B and 4C of the main text). Based on results, the stimulation of cells with $H_2O_2$ at 100 μM for 2 h was fixed as the standard procedure for having $H_2O_2$-induced HUVEC cells.

**S5.2. Viability assays**. The cytotoxicity of the free DSeU, ZIF8 and DSeU@ZIF8 particles was investigated by using two different cell viability assays as follows. Note that although WST-1 and MTT assays are similar in principle, as both measures the metabolic activity of viable cells, however, the WST-1 assay produces a water-soluble formazan, eliminating thus the additional solubilization step. In this regard, the WST-1 assay is faster and, most importantly, allows monitoring the cell viability in the same well over time, simplifying studies at different times.

***MTT assay***: Cells were seeded in completed medium in 96-well plates at a density of 15,000 cells/well for 24 h. Prior to each experiment, the diluted suspensions of

compound/particles were freshly prepared in serum-free culture medium. After that 24 h, the medium was removed, and serum-free medium containing different concentrations of the compound/particles (within the range of DSeU concentration 1 – 50 µM, or the equivalent particles concentration range of 8.2 – 412 µg/mL) was added to cells. Untreated cells were used as the control. At the end of the incubation period for 24 h, the treatment solutions were removed, and cells were washed twice with PBS. Next, a solution of 50 µL of media containing MTT at 1 mg/mL (MTT is [3-(4,5-dimethylthiazol-2-yl)-2,5-diphenyltetrazolium bromide, AppliChem Panreac) was added to the wells, and plates were incubated at 37 °C in 5% $CO_2$ for 2 h. After incubation, the media was replaced and the formazan crystals were diluted in 100 µL of isopropanol. Cell viability was assessed by measuring absorbance at 570 nm (reference 650 nm) using microplate reader. Viability was determined as a percentage of control (viability of control cells was set as 100%).

***WST-1 assay***: Cells were seeded in completed medium in 96-well plates at a density of 15,000 cells/well for 24 h. Cells were treated as indicated above. After treatment, the culture medium was replaced with 100 µL of serum- and phenol red-free medium, following by the addition of 10 µL of pure WST-1 (Roche) per well. After 2h incubation at 37ºC and 5% $CO_2$, absorbance was measured at wavelength 450 nm for samples and 600 nm for background using a microplate reader. Cell viability was calculated by subtracting the background absorbance values from the resulting values of the samples.

**S5.3. Cell uptake study**. Fluorescent rhodamine B-loaded DSeU@ZIF8 particles (RhB@DSeU@ZIF8) were prepared (see section S3.1) to easily monitor the particles by confocal microscopy. HUVEC cells were first seeded in 96-well plates and incubated for 24 h. Then, RhB@DSeU@ZIF8 particles (at particles concentration of 8.2 µg/mL, which contain 1 µM of DSeU; suspensions prepared in serum-free culture medium without phenol red just before the assay) were added to the cells, and live-cells images were taken at different incubation times (1 h, 6 h and 24 h) as shown in Fig. 3C and Fig. S17. Control experiments without addition of particles were also performed to establish the imaging settings according to the potential fluorescent background. The mean fluorescence intensity per cell was calculated the imaging software Aivia v12 and Cellpose plug-in (Leica Microsystems), Fig. 3C and Fig. S19.

**S5.4. ROS assay**. The intracellular ROS level was determined using 2′,7′-dichlorfluorescein-diacetate (DCFH-DA, Sigma–Aldrich), a cell membrane-permeable fluorogenic probe that measures the activity of hydroxyl, peroxyl and other ROS species. Thus, this probe reflects the overall oxidant status in cells and is widely used as a marker of oxidative stress. DCFH-DA can react with the different oxidant molecules belonging to the ROS family, and the product dichlorofluorescein (DCF) can be excited at 485 nm with the maximum emission intensity at 535 nm. The fluorescence intensity increases in proportion to the level of cellular oxidants and is expressed as percent increase *vs* basal values (i.e., ROS level in untreated cells). The optimized protocol for this assay was as follows. HUVEC cells were first seeded in 96-well plates and incubated for 24 h. Then, different concentrations of the free DSeU, ZIF8 particles or DSeU@ZIF8 particles (suspensions prepared in serum-free culture medium just before the assay) were added and incubated for 24 h; except in the experiments in which the antioxidant activity of the particles as a function of incubation time was investigated (Figure S12B), in which this

incubation time varied as indicated. At the end of the incubation period, the treatment solutions were removed, and cells were washed twice with PBS in order to remove the fraction of particles or compound non-internalized in cells. Afterwards, the DCFH-DA probe (100 µL at a final concentration of 25 µM) was added and incubated for 30 min at 37 °C in 5% $CO_2$ before the further challenge with the specific stimulus. For the experiments to study the antioxidant activity of the compound/particles in the absence of $H_2O_2$ as the stimulus, the fluorescence was measured just after the 24 h incubation period with the DCFH-DA probe. For studies to investigate the capability of the compound/particles to counteract the oxidative stress caused by the $H_2O_2$ stimulus, after the incubation of cells with DCFH-DA for 30 min, $H_2O_2$ was added at a final concentration of 100 mM and the fluorescence measurements were carried out after 2 h of incubation (unless otherwise specified as in the case of optimization studies for selecting the optimal concentration/time for the stimulus treatment; Figures 4B-C of the main text).

**S5.5. Angiogenesis assay**. This assay was used to evaluate the potential of HUVECs to form vascular structures, and was performed on Matrigel substrate using the Cell Biolabs Endothelial Tube Formation test kit (Cell Biolabs, San Diego, CA, USA). Again, cells were subjected to two different treatments: (1) cells stimulated with $H_2O_2$ (100 µM, 2 h) to induce oxidative stress-injury, and (2) cells pre-treated with DSeU@ZIF8 particles (1 µM, 24 h), the medium was then removed, cells washed twice with PBS, and then exposed to $H_2O_2$ (100 µM, 2 h). Then, 96-well plates were coated with 50 µL gel solution at 4 ºC and incubated at 37 °C and 5% $CO_2$ for 30 min. Endothelial cells were trypsinized, and $10^4$ cells/well were seeded on the Matrigel. After 2 h, photographs were taken with an optical inverted microscope. Length of tube-like structures per field was quantified with “angiogenesis analyzer” and an automated analysis was performed with the ImageJ software.

**S5.6. Wound healing assay**. This assay aims to study 2D cell migration, allowing to evaluate the impact of different treatments on the wound-healing and tissue reparation capabilities of cells. Cells were exposed to two different conditions: (1) cells stimulated with $H_2O_2$ (100 µM, 2 h) to induce oxidative stress-injury, and (2) cells pre-treated with DSeU@ZIF8 particles (1 µM, 24 h), the medium was then removed, cells washed twice with PBS, and then exposed to $H_2O_2$ (100 µM, 2 h). After treatments, the cell monolayer in each well was scratched across the centre using a sterile micropipette tip. Subsequently, cells were rinsed with PBS to discard the cellular debris detached from the "wound" zone. Next, complete medium was added and cells were incubated at 37 °C and 5% $CO_2$. The wound images were captured by optical microscopy (OPTIKA Microscopes) at t=0 and 6 h, and the wound area was determined using ImageJ software.

**S5.7. Statistical analysis**. Quantitative variables were expressed as mean ± standard deviation (SD) of three independent experiments. Data distribution was analyzed with the Shapiro-Wilk test to verify a normal distribution. The difference between means for two different groups was assessed by Student´s t test. The difference between means for three groups was determined by ANOVA with Bonferroni post-hoc correction. p values of less than 0.05 were considered as significant. Data were analyzed using SPSS Statistics software version 25.0 (SPSS, Inc., Chicago, IL, USA).

## S5.8. Additional figures and tables with statistic data

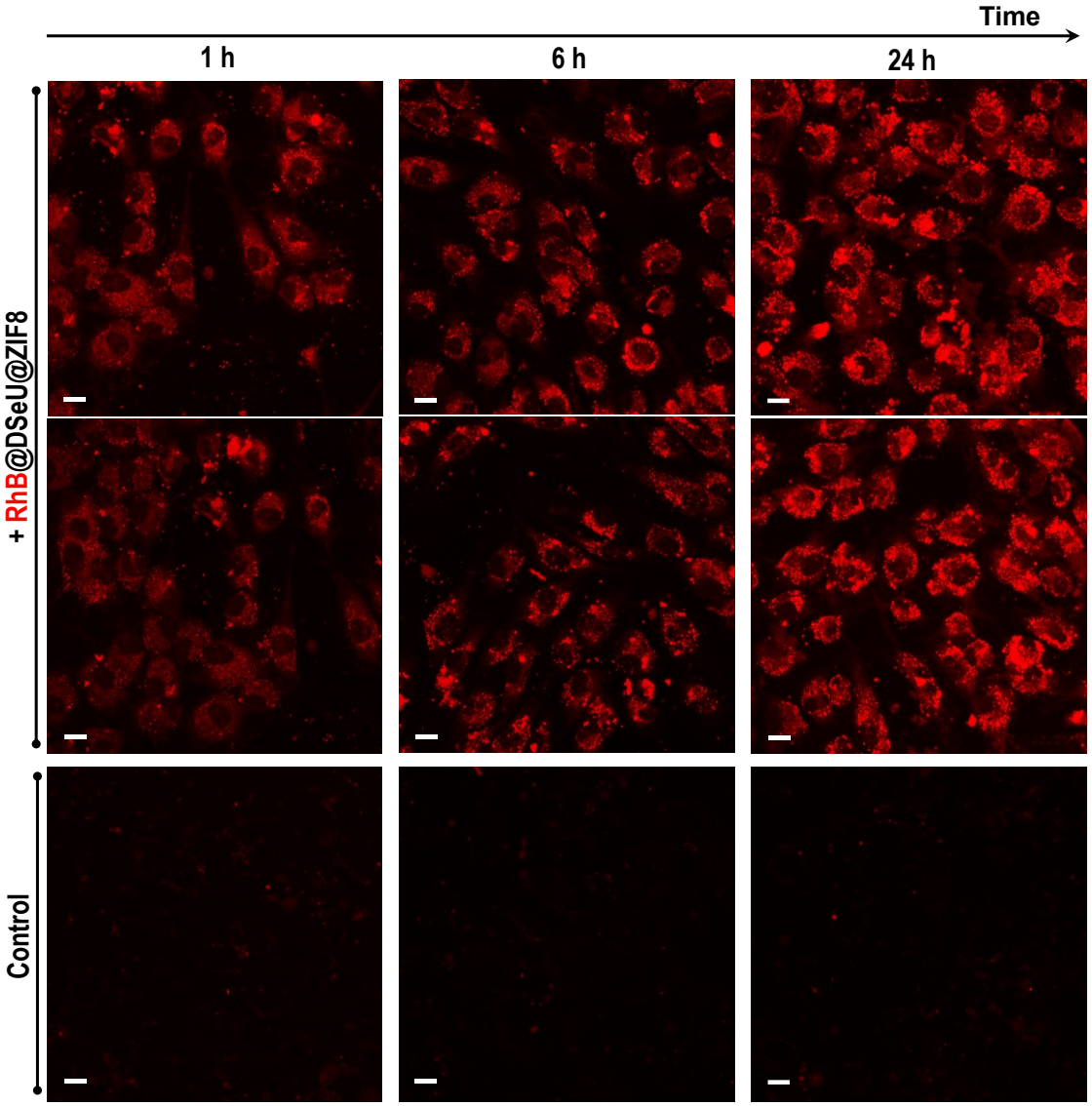


**Figure S17**. Cellular uptake of fluorescent RhB@DSeU@ZIF8 particles. Confocal laser scanning microscopy images at 40x magnification of HUVEC cells incubated with RhB@DSeU@ZIF8 (8.2 μg/mL, expressed as particles concentration) for 1 h, 6 h or 24 h, and cells without particles acting as negative control. Red fluorescence channel for RhB ($\lambda_{ex}$=514 nm, $\lambda_{em}$=575-650 nm) is shown. Scale bars correspond to 10 μm.

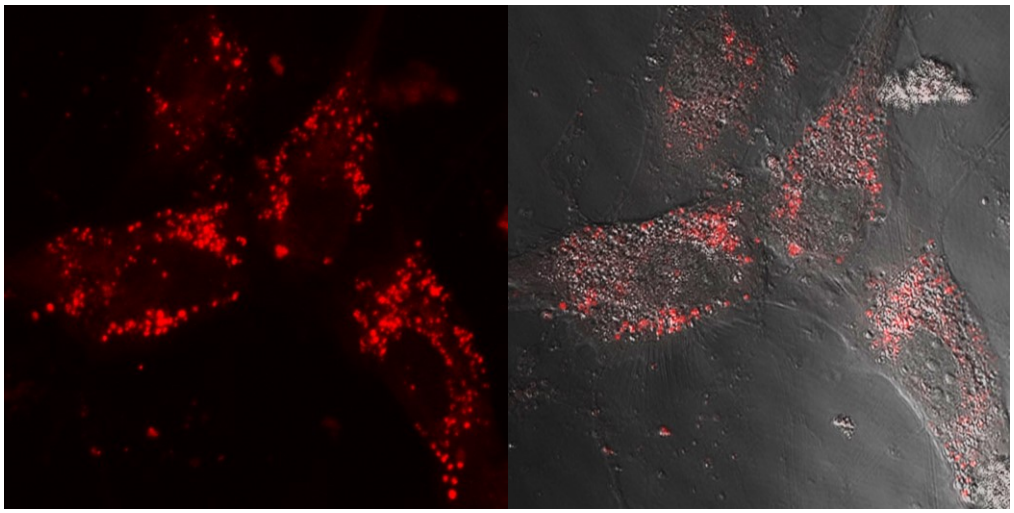

**Figure S18**. Confocal microscopy image at 63x magnification of HUVEC cells incubated with RhB@DSeU@ZIF8 (8.2 µg/mL) for 24 h. Red fluorescence channel (left) and merge with the bright field (right) are shown.

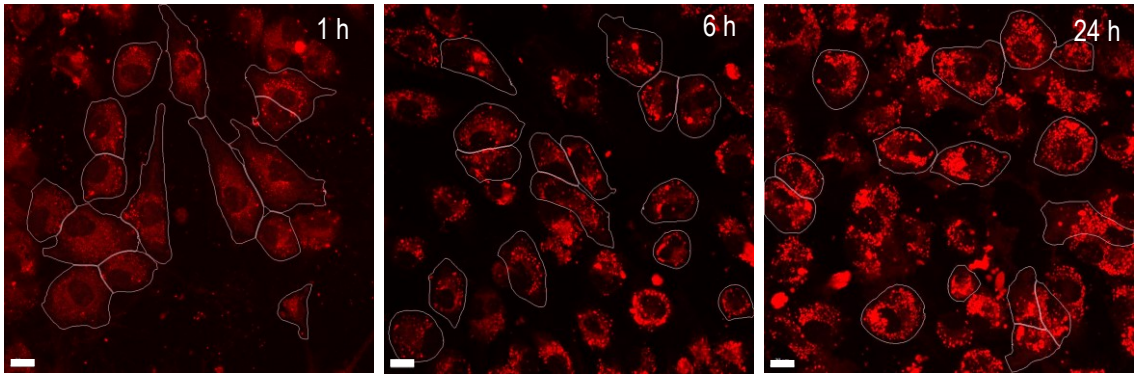


**Figure S19**. Cell segmentation using the Cellpose plug-in included in the imaging software Aivia v12 (Leica Microsystems).

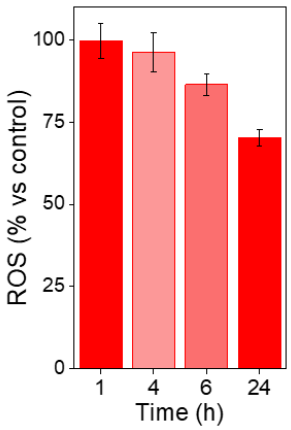


**Figure S20.** Intracellular ROS (% *vs* control) of cells incubated for different times with DSeU@ZIF8 particles (8.2 µg/mL of particles concentration that contain 1 µM of DSeU). Untreated cells are considered as control cells, from which the basal ROS level is determined. Data expressed as the mean ± SD of three independent experiments.

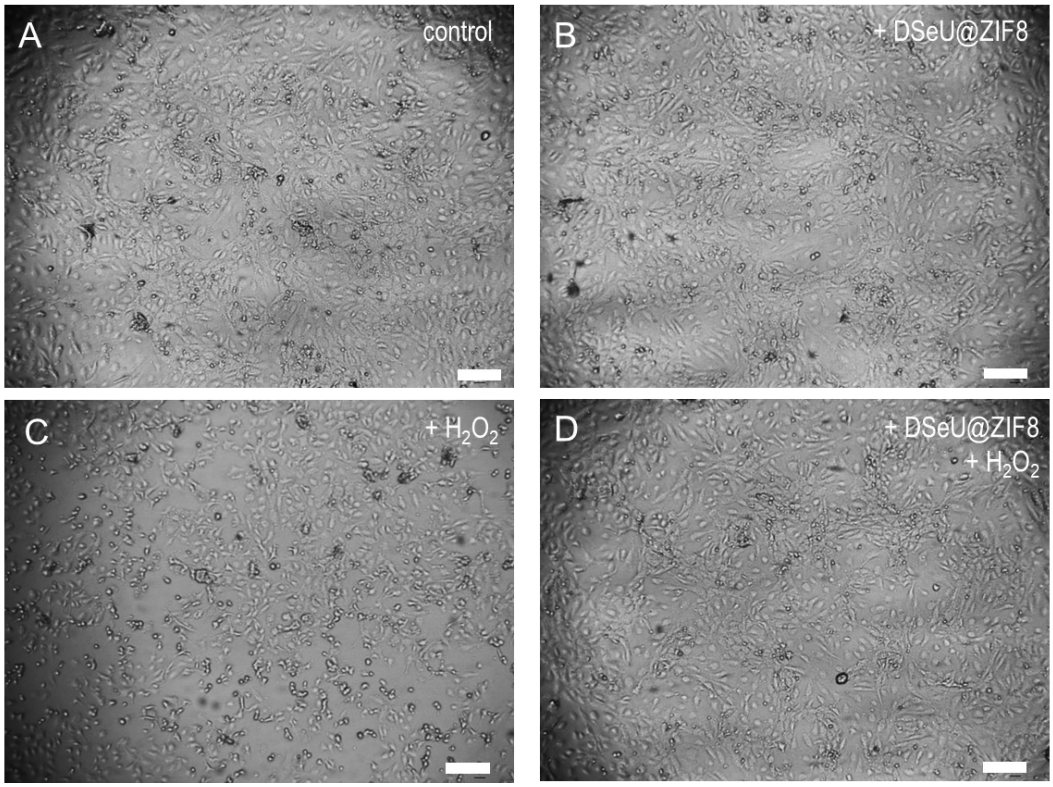


**Figure S21.** Representative images of inverted optical microscopy of HUVEC cells after different treatments: (A) untreated cells (negative control); (B) after 24 h exposure to 1 μM of DSeU@ZIF8 particles; (C) cells stimulated with 100 μM $H_2O_2$ for 2 h (positive control); (D) cells incubated first with DSeU@ZIF8 (1 μM, 24 h), followed by treatment with $H_2O_2$ (100 μM, 2 h). Scale bars correspond to 200 μm.

**Table S5.** Statistics for data in Figure 3D.

| **Bonferroni's multiple comparisons test** | | | | | |
|---|---|---|---|---|---|
| **DSeU@ZIF8** | ***p value*** | **DSeU** | ***p value*** | **ZIF8** | ***p value*** |
| 0.5μM *vs* 1μM | 0.0177 | 0.5μM *vs* 1μM | ns* | 0.5μM *vs* 1μM | ns* |
| 0.5μM *vs* 2μM | 0.0005 | 0.5μM *vs* 2μM | ns* | 0.5μM *vs* 2μM | 0.0486 |
| 1μM *vs* 2μM | 0.0186 | 1μM *vs* 2μM | ns* | 1μM *vs* 2μM | ns* |

| **Bonferroni's multiple comparisons test** | | | | | |
|---|---|---|---|---|---|
| **0.5 μM** | ***p value*** | **1 μM** | ***p value*** | **2 μM** | ***p value*** |
| DSeU@ZIF8 *vs* DSeU | 0.027 | DSeU@ZIF8 *vs* DSeU | 0.001 | DSeU@ZIF8 *vs* DSeU | 0.0006 |
| DSeU@ZIF8 *vs* ZIF8 | ns* | DSeU@ZIF8 *vs* ZIF8 | 0.0059 | DSeU@ZIF8 *vs* ZIF8 | 0.0038 |
| DSeU *vs* ZIF8 | ns* | DSeU *vs* ZIF8 | ns* | DSeU *vs* ZIF8 | ns* |

*ns = not statistically significant

**Table S6.** Statistics for data in Figure 4D.

| **Bonferroni's multiple comparisons test** | | | | | | | |
|---|---|---|---|---|---|---|---|
| **Cnt-** | **Cnt-** | | | | | | |
| **Cnt+** | <0.0001 | **Cnt+** | | | | | |
| **0.5 h** | <0.0001 | <0.0001 | **0.5 h** | | | | |
| **1 h** | <0.0001 | <0.0001 | <0.0001 | **1 h** | | | |
| **1.5 h** | <0.0001 | <0.0001 | <0.0001 | <0.0001 | **1.5 h** | | |
| **2 h** | <0.0001 | <0.0001 | <0.0001 | <0.0001 | <0.0001 | **2 h** | |
| **3 h** | <0.0001 | <0.0001 | <0.0001 | <0.0001 | <0.0001 | <0.0001 | **3 h** |
| **4 h** | <0.0001 | <0.0001 | <0.0001 | <0.0001 | <0.0001 | <0.0001 | <0.0001 |

**Table S7.** Statistics for data in Figure 4E.

| **Bonferroni's multiple comparisons test** | | | | |
|---|---|---|---|---|
| **Cnt-** | **Cnt-** | | | |
| **DSeU@ZIF8** | 0.004 | **DSeU@ZIF8** | | |
| **Cnt+** | 0.009 | 0.004 | **Cnt+** | |
| **DSeU@ZIF8+$H_2O_2$** | 0.003 | <0.0001 | 0.003 | **DSeU@ZIF8+$H_2O_2$** |